Temperature dependence of thermodynamic properties for DNA/DNA and RNA/DNA duplex formation

Peng Wu[1],[*], Shu-ichi Nakano[1] and Naoki Sugimoto[1],[2]

[1]*High Technology Research Center and* [2]*Department of Chemistry, Faculty of Science and Engineering, Konan University, Okamoto, Higashinada–ku, Japan*

A clear difference in the enthalpy changes derived from spectroscopic and calorimetric measurements has recently been shown. The exact interpretation of this deviation varied from study to study, but it was generally attributed to the non-two-state transition and heat capacity change. Although the temperature-dependent thermodynamics of the duplex formation was often implied, systemic and extensive studies have been lacking in universally assigning the appropriate thermodynamic parameter sets. In the present study, the 24 DNA/DNA and 41 RNA/DNA oligonucleotide duplexes, designed to avoid the formation of hairpin or slipped duplex structures and to limit the base pair length less than 12 bp, were selected to evaluate the heat capacity changes and temperature-dependent thermodynamic properties of duplex formation. Direct comparison reveals that the temperature-independent thermodynamic parameters could provide a reasonable approximation only when the temperature of interest has a small deviation from the mean melting temperature over the experimental range. The heat capacity changes depend on the base composition and sequences and are generally limited in the range of -160 to ≈ -40 cal·mol^{-1}·K^{-1} per base pair. In contrast to the enthalpy and entropy changes, the free energy change and melting temperature are relatively insensitive to the heat capacity change. Finally, the 16 NN-model free energy parameters and one helix initiation at physiological temperature were extracted from the temperature-dependent thermodynamic data of the 41 RNA/DNA hybrids.

Keywords: heat capacity change; temperature-dependent thermodynamics; enthalpy-entropy compensation; the NN-model parameters.

With the dramatic progress in the human genome project, many gene sequences are well known but their structure and function are not yet clearly understood, and therefore, thermodynamic optimization strategy plays more and more important role in understanding and predicting the sequence-dependent higher-ordered structures of nucleic acids [1–4]. Knowledge of the thermodynamics of nucleic acids will also be very useful for designing appropriate screening or scanning experiments for identifying the genetic markers for diseases [5], sequencing single nucleotide polymorphisms on a genome-wide scale [6], calculating hybridization equilibria for purposes of designing the PCR and rolling-cycle amplification [7,8], selecting optimal conditions for hybridization experiments, and determining the minimum length of a probe required for the hybridization and cloning experiments [9,10]. Moreover, the development of DNA chips for rapidly screening and sequencing unknown DNAs mainly relies on the ability to predict the thermodynamic stability of the complexes formed by the oligonucleotide probes [11,12].

Spectroscopic and calorimetric measurements are two widely applied methods to determine the thermodynamic parameters of nucleic acids [13–15]. The UV measurement is highly sensitive and only small sample units are required for a full set of measurements on a nucleotide sequence; as a result, this method has been implemented in many different ways and applied as a standard way to construct the thermodynamic database of oligonucleotide sequences [16–25]. The calorimetric measurement offers the directly determined thermodynamic parameters of nucleotide sequences, but this approach requires a substantially larger sample size for a full set of measurements on a nucleotide sequence. When the van't Hoff enthalpy derived from the UV measurements was directly compared with the calorimetric enthalpy derived from the calorimetry measurements, it was often found that the two quantities disagreed with each other and this difference in the two enthalpies sometimes approached 100% [26–35]. This appears to be a general problem that has been recently addressed by several labs, all with slightly different emphases and different conclusions [26–31,36,37]. The possible interpretation is that

Correspondence to N. Sugimoto, Department of Chemistry, Faculty of Science and Engineering, Konan University, Kobe 658-8501, Japan.
Fax: + 81 78 4352539, Tel.: + 81 78 4352497,
E-mail: sugimoto@konan-u.ac.jp

Definitions: A, the absorbance of a solution at any temperature; A_{helix}, the linear absorbance as a function of temperature in the pretransition process; A_{coil}, the linear absorbance as a function of temperature in the post-transition process; T_{m}, melting temperature; ΔC_{p}, heat capacity change; $\Delta C_{\text{p,H}}$, the heat capacity change in enthalpy derived from a linear regression of enthalpy change with respect to melting temperature ($\Delta C_{\text{p,H}} = d\Delta H/dT_{\text{m}}$); $\Delta C_{\text{p,S}}$, the heat capacity change in entropy derived from a linear regression of entropy change with respect to the logarithmic scale of melting temperature ($\Delta C_{\text{p,S}} = d\Delta S/d\ln T_{\text{m}}$); T^0, the reference temperature; ΔH^0, the enthalpy change in the reference state; ΔS^0, the entropy change in the reference state; NN-model, the nearest-neighbor model.

[*]*Present address*: Department of Chemistry, The Pennsylvania State University, University Park, PA 16802, USA.

the helix-to-coil melting is a non-two-state transition [27,30,32] and the difference in hydration between the duplex-stranded groups and single-stranded groups results in a heat capacity increase [26–29,34,37–42]. It should be noted that for short oligonucleotide sequences, the duplex formation behaves in a two-state transition [17,43], while for longer oligonucleotide sequences, the duplex formation often behaves as a non-two-state transition due to the self-assembled population of single strands [27,30]. Although the change in heat capacity was generally regarded as a dominant factor for the difference between the van't Hoff enthalpy and the calorimetric enthalpy [28,29,36–38], the effect of heat capacity change on the thermodynamic properties of duplex formation, except for a few studies [39–42], has been lacking. Therefore, systemic and extensive investigations are still required to assign universally appropriate parameter sets of the temperature-dependent thermodynamics for the DNA/DNA and RNA/DNA oligonucleotide duplexes.

In the present study, we determined the temperature-independent and temperature-dependent thermodynamic parameters of 24 DNA/DNA and 41 RNA/DNA oligonucleotide duplexes. The heat capacity changes were derived by two methods: a linear regression of enthalpy with respect to the melting temperature ($\Delta C_{p,H} = d\Delta H/dT_m$) and a linear regression of entropy with respect to the logarithmic scale of the melting temperature ($\Delta C_{p,S} = d\Delta S/d\ln T_m$). The thermodynamic properties of the duplex formation determined by $\Delta C_P = 0$ and $\Delta C_P \neq 0$ were extensively discussed and compared. The compensation of the temperature-dependent enthalpy and entropy was also taken into account. Finally, the 16 NN-model free energy parameters and one helix initiation at physiological temperature were extracted from the temperature-dependent thermodynamic data of the 41 RNA/DNA hybrids. These observations provide a thorough insight into the origin of the duplex association/dissociation transition.

MATERIALS AND METHODS

Material preparations

DNA and RNA oligonucleotides were synthesized on a solid support using the standard phosphoramidite method with an Applied Biosystems Model 391 synthesizer and purified by RP-HPLC with Wakosil-II 5C18RS cartridges after de-blocking operations, then the oligonucleotides were aliquoted for the UV melting experiments. The final purity of these oligonucleotides was greater than 95%. All experiments were carried out in a buffer solution containing 1 M NaCl/10 mM Na$_2$HPO$_4$/1 mM Na$_2$EDTA (pH 7.0). The single strand concentrations of the oligonucleotides were determined by measuring the absorbance (260 nm) at a high temperature. Two complementary single strands were mixed in an equimolar ratio to form a duplex.

UV melting measurements

UV thermal scans with single and duplex strands were performed on Hitachi U-3200 and U-3210 spectrophoto-

meters equipped with a Hitachi SPR-7 and SPR-10 thermoprogrammer and temperature probes. All melting curves of the duplex denaturation were collected at a 260-nm wavelength as a function of temperature over the range from 0 to 95 °C. Prior to the melting experiments, the samples were first heated to 95 °C for 20 min and then slowly annealed to the starting temperature of each heating-cooling cycle. The water condensation on the cuvette exterior in the low temperature region can be avoided by flushing with a constant stream of dry nitrogen. The heating rates were fixed at 0.5 or 1.0 °C·min^{-1} based on the cuvette length. For each oligonucleotide duplex, at least seven individual scans were performed to determine the thermodynamic parameters.

Temperature-independent thermodynamic analysis

To provide the maximum likelihood of a two-state pattern for the duplex association/dissociation transition, all the oligonucleotide sequences were designed to avoid the formation of hairpin or slipped duplex structures and to limit the base pair length less than 12 bp. For any of the non-self-complementary duplex formations, the thermodynamic parameters can be determined by two conventional van't Hoff analysis methods. One is to plot the reciprocal of the melting temperature (in Kelvin), T_m^{-1}, vs. $\ln(C_T/4)$ using the van't Hoff equation [19,24,25,39–42]:

$$T_m^{-1} = \frac{R}{\Delta H} \ln \frac{C_T}{4} + \frac{\Delta S}{\Delta H} \qquad (1)$$

where ΔH and ΔS are the enthalpy and entropy changes, respectively. T_m is melting temperature. C_T is the total species concentration and R is the gas constant, 1.987 cal·K^{-1}mol^{-1}. Another method is to fit the shape of the melting curves by using nonlinear least-squares program. In all cases, the absorbance as a function of temperature in the course of duplex melting can be given by [22,39,44–47]:

$$A(T) = (1 - \alpha) \times A_{helix}(T) + \alpha \times A_{coil}(T) \qquad (2)$$

where $A(T)$ is the absorbance of a solution at the temperature of interest. $A_{helix}(T)$ and $A_{coil}(T)$ are defined as the sloped linear baselines of the melting curves in the helix and coil states, respectively [45,47]. That is:

$$A_{helix}(T) = b_{ds} + m_{ds} \times T \qquad (3)$$

$$A_{coil}(T) = b_{ss} + m_{ss} \times T \qquad (4)$$

where b_{ds}, b_{ss}, m_{ds}, and m_{ss} are the intercepts and slopes of the lower and upper baselines of the melting curves, respectively; T is the temperature of interest in Kelvin, α is the molar fraction of strands in the coiled state and can be written as:

$$\alpha = 1 + \frac{1 - \sqrt{2C_T \exp[(-\Delta H + T\Delta S)/(RT)] + 1}}{C_T \exp[(-\Delta H + T\Delta S)/(RT)]} \qquad (5)$$

The enthalpy and entropy changes of each transition, as the estimated parameters, are determined by the best fit to the shape of the melting curves according to Eqns (2)–(5). The resulting enthalpy change and entropy changes are obtained by averaging all the fitted values at the different concentrations. It should be noted that the above two methods imply the assumption of $\Delta C_p = 0$ [19–25,44–48].

Temperature-dependent thermodynamic analysis

The differences in hydration between the structured duplex strand and the coiled single strands gives rise to an increase in the heat capacity [27,49–52], resulting in a clear temperature dependence of the enthalpy and entropy changes [36–42]. With respect to the reference state, the enthalpy and entropy changes as a function of temperature are given by [14,28,39,53–56]:

$$\Delta H(T_{m}) = \Delta H^0 + \int_{T^0}^{T}\Delta C_{p,H}dT$$
$$= \Delta H^0 + \Delta C_{p,H}(T_m - T^0) \qquad (6)$$

$$\Delta S(T_{m}) = \Delta S^0 + \int_{T^0}^{T}\Delta C_{p,S}d\ln T$$
$$= \Delta S^0 + \Delta C_{p,S}\ln(T_m/T^0) \qquad (7)$$

where ΔH and ΔS are the enthalpy and entropy changes at the temperature of interest, ΔH^0 and ΔS^0 are the enthalpy and entropy changes in the reference state, T^0 is the reference temperature, $\Delta C_{p,H}$ is the heat capacity change in enthalpy derived from a linear regression of the enthalpy change with respect to the melting temperature ($\Delta C_{p,H} = d\Delta H/dT_m$), and $\Delta C_{p,S}$ is the heat capacity change in entropy derived from a linear regression of the entropy change with respect to the logarithmic scale of the melting temperature ($\Delta C_{p,S} = d\Delta S/d\ln T_m$). In principle, the heat capacity changes determined by the above two methods should be equivalent. However, Rouzina & Bloomfield analyzed the published data on ΔH and ΔS of the duplex formation and revealed that there were always differences between $\Delta C_{p,H}$ and $\Delta C_{p,S}$ [28]. Such differences in heat capacity change were theoretically confirmed and the arithmetic mean value, $\Delta C_p^{ave} = (\Delta C_{p,H} + \Delta C_{p,S})/2$, was suggested [28]. These observations are further confirmed by recent studies [55]. Thus, the free energy change at the temperature of interest can be written as [54]:

$$\Delta G(T_{m}) = \Delta H^0(1 - T_m/T^0)$$
$$+ \Delta C_p^{ave}[T_m - T^0 - T_m\ln(T_m/T^0)] \quad (8)$$

The mean values of thermodynamic parameters

For $\Delta C_p = 0$, the statistical mean values of the enthalpy and entropy changes, ΔH^{mean} and ΔS^{mean}, are simply given by:

$$\Delta H^{mean} = \frac{\sum_{i=1}^{m}\Delta H_i}{n} \qquad (9)$$

$$\Delta S^{mean} = \frac{\sum_{i=1}^{m}\Delta S_i}{n} \qquad (10)$$

where ΔH_i and ΔS_i are the enthalpy and entropy changes at each concentration. n is the number of measurements.

For $\Delta C_P \neq 0$, $\Delta H(T)$ and $\Delta S(T)$ should be taken as a continuous function of the melting temperature on the temperature interval $[T_{min}, T_{max}]$ (Eqns 6 and 7), as a result, the mean values of the temperature-dependent enthalpy and entropy changes can be written as:

$$\Delta H^{mean} = \Delta H^0 + \Delta C_P^{ave}(T_{mean} - T^0) \qquad (11)$$

$$\Delta S^{mean} = \Delta S^0 + \Delta C_P^{ave}\ln(T_{mean}/T^0) \qquad (12)$$

where T_{min} and T_{max} are the minimum and maximum temperatures over the experimental temperature range, respectively. T_{mean} is the arithmetic mean value of T_{min} and T_{max}, i.e. $T_{mean} = (T_{min} + T_{max})/2$. Likewise, the melting temperature at the concentration of interest, C_T, can be given by:

$$T_{m} = \frac{\Delta H^0 + \Delta C_p^{ave}(T_m - T^0)}{R\ln(C_T/4) + \Delta S^0 + \Delta C_p^{ave}\ln(T_m/T^0)} \quad (13)$$

RESULTS AND DISCUSSION

Temperature-independent thermodynamic parameters

In contrast to the temperature-dependent thermodynamic parameters of the 24 DNA/DNA and 41 RNA/DNA oligonucleotide duplexes (Table 1), the temperature-independent thermodynamic parameters (data not shown) clearly depend on the experimental temperature range. Direct comparison of the two parameter sets revealed that the temperature-independent thermodynamic parameters could provide a reasonable approximation only when the temperature of interest deviates only slightly from the mean melting temperature over the experimental range (data not shown).
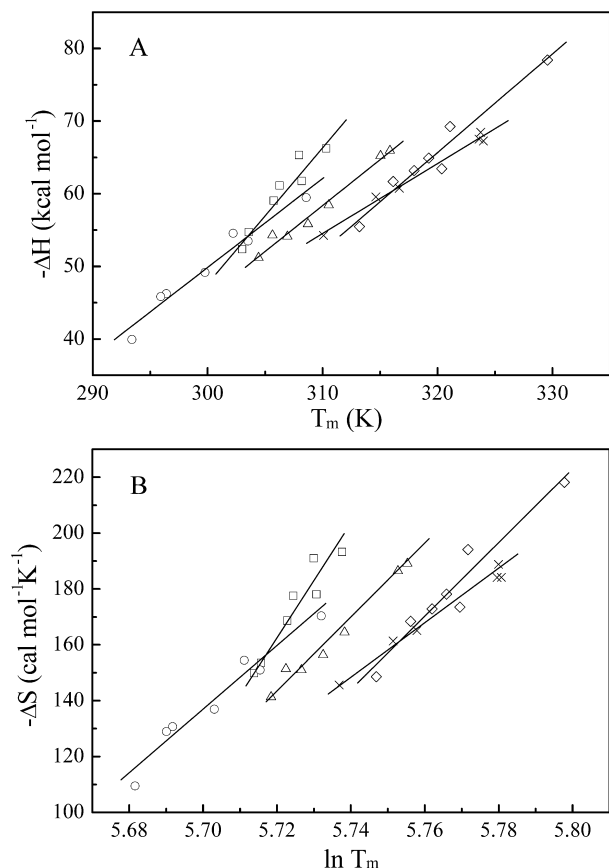
Heat capacity change

It is well known that the heat capacity change is the net sum of the positive contribution from the exposure of nonpolar groups and the negative contribution from the exposure of polar groups [49,51]. When the structured double strand is melted into the coiled single strands, the difference in hydration between the different strands results in an increase of the heat capacity. This heat capacity change is related to the ratio of the nonpolar to polar buried surface in an oligonucleotide duplex [27,49–52]. Figures 1 and 2 show the representative plots of temperature dependence of the enthalpy and entropy changes for the different base-pair compositions and sequence lengths. As the perturbation contributed from the enthalpy and entropy changes might be different in the course of duplex melting, the heat capacity change in enthalpy, $\Delta C_{p,H}$, is not always in agreement with the heat capacity change in entropy, $\Delta C_{p,S}$, as summarized in Table 1. Nevertheless, these differences are mostly limited to 5%. Recently, Rouzina & Bloomfield theoretically confirmed that the difference between $\Delta C_{p,H}$ and $\Delta C_{p,S}$ should equal the transition entropy [28]. The current experimental studies strongly support this conclusion [55]. Similar reports have also been seen in previous studies [39]. This insight suggests that the extent of enthalpy and entropy changes along with temperature might be different in the real course of the duplex melting. The heat capacity change depends somewhat on the base-pair compositions and sequences; the mean values are generally limited in the range −160 to −40 cal·mol^{-1}·K^{-1} per base-pair (see Fig. 3), consistent with the previous spectroscopic [28,39–42,55,56] and calorimetric measurements [27,34,36]. Additionally, the current studies further

Table 1. Heat capacity changes and temperature-dependent thermodynamic parameters of DNA complexes. Only the top sequences are shown and all the complementary sequences are DNA strands. All experiments were carried out in a buffer containing 1 M NaCl/10 mM Na$_2$HPO$_4$/1 mM Na$_2$EDTA (pH 7.0). Temperature range indicates the melting temperatures over the entire experimental range. $\Delta C_{p,H}$ is the heat capacity change in enthalpy derived from a plot of ΔH vs. T_m. $\Delta C_{p,H} = d\Delta H/dT_m$. $\Delta C_{p,s}$ is the heat capacity change in entropy derived from plot of ΔS vs. ln T_m. $\Delta C_{p,s} = d\Delta S/d\ln T_m$. ΔC_p^{ave} are the arithmetic mean value of $\Delta C_{p,H}$ and $\Delta C_{p,s}$. The temperature-dependent thermodynamic parameters at 25 °C and at 37 °C are estimated by Eqns (6)–(8). T_m was calculated by Eqn (13) at a total species concentration of 100 µM.

	Temperature range (°C)	Heat capacity change			Thermodynamic parameters at 37 °C			Thermodynamic parameters at 25 °C			T_m (°C)
		$-\Delta C_{p,H}$ (kcal·mol^{-1}·K^{-1})	$-\Delta C_{p,s}$ (kcal·mol^{-1}·K^{-1})	$-\Delta C_p^{ave}$ (kcal·mol^{-1}·K^{-1})	$-\Delta H_{37}$ (kcal·mol^{-1})	$-\Delta S_{37}$ (cal·mol^{-1}·K^{-1})	$-\Delta G_{37}$ (kcal·mol^{-1})	$-\Delta H_{25}$ (kcal·mol^{-1})	$-\Delta S_{25}$ (cal·mol^{-1}·K^{-1})	$-\Delta G_{25}$ (kcal·mol^{-1})	
DNA/DNA											
dAGCCCG/d	20.4–34.1	0.46	0.41	0.43	45.9	129.4	5.74	40.4	113.2	6.64	31.6
dCGTGC/d	20.5–33.9	0.62	0.59	0.61	48.2	137.6	5.48	40.7	114.2	6.68	30.1
dCGGTGC/d	30.8–44.6	0.94	0.96	0.95	57.9	164.3	6.99	46.7	126.5	8.98	39.4
dCACGGC/d	26.1–44.9	2.04	1.94	1.99	68.0	196.0	7.21	43.6	119.4	7.97	40.0
dACCGCA/d	21.6–39.3	0.28	0.27	0.28	41.0	110.8	6.67	37.6	100.1	7.78	38.0
dAATACCG/d	19.1–33.0	0.89	0.88	0.88	54.3	157.7	5.39	43.7	123.0	6.99	30.3
dAGCTTCA/d	19.9–36.2	0.86	0.84	0.85	52.8	150.8	5.99	42.4	117.5	7.36	33.8
dAGCCGTG/d	35.8–48.7	0.70	0.70	0.70	49.8	133.7	8.31	41.4	106.1	9.79	47.7
dGGATTGA/d	15.1–30.2	0.94	0.92	0.93	55.8	162.4	5.39	44.5	126.0	6.88	30.4
dACCTAGTC/d	26.9–40.0	1.46	1.53	1.51	57.7	164.8	6.59	39.9	104.5	8.70	37.3
dCTAGTGGA/d	30.6–42.9	0.66	0.69	0.68	50.6	140.4	7.07	42.6	113.1	8.93	40.3
dGTCGAACA/d	33.9–45.5	0.38	0.40	0.39	54.6	149.7	8.15	50.1	134.0	10.11	46.2
dCGCAGTTA/d	35.0–49.4	0.66	0.65	0.66	49.8	135.0	7.93	41.9	109.2	9.32	45.5
dCGCTGTAA/d	31.4–43.9	0.32	0.31	0.32	49.8	136.2	7.53	45.9	123.8	8.96	43.2
dCACGGCTC/d	42.3–53.1	0.35	0.42	0.39	52.8	137.2	10.22	48.6	120.6	12.61	58.5
dAATCCAGT/d	26.5–40.5	0.28	0.27	0.28	52.0	145.8	6.76	48.6	135.0	8.34	38.4
dAGTCCTGA/d	24.4–40.4	0.70	0.69	0.70	48.8	133.2	7.45	40.4	105.9	8.77	42.7
dACGACCTC/d	35.9–47.5	0.42	0.41	0.42	55.2	150.5	8.53	50.1	134.5	10.04	48.2
dCTCACGGC/d	39.9–51.2	0.97	1.01	0.99	47.3	123.2	9.14	35.7	83.4	10.79	52.5
dAGCGTAAG/d	31.6–44.7	0.38	0.38	0.38	47.8	130.2	7.37	43.2	115.4	8.81	42.4
dATCTATCCG/d	37.8–46.7	1.03	1.11	1.07	54.7	148.5	8.59	42.3	104.9	11.03	48.0
dGCCAGTTAA/d	37.0–47.6	0.11	0.12	0.12	61.1	169.6	8.53	59.8	164.9	10.59	47.4
dGCCAGTTAT/d	38.9–48.5	0.76	0.81	0.78	57.2	155.8	8.91	48.2	123.9	11.20	49.4
dGCATAATACGT/d	42.9–52.5	0.05	0.10	0.08	74.6	206.1	10.72	74.0	202.0	13.76	55.5
RNA/DNA											
rCGGCU/d	15.2–30.4	0.21	0.19	0.20	49.9	141.9	5.93	47.4	134.3	7.34	33.3
rAGCCG/d	24.9–38.7	0.68	0.68	0.68	49.7	141.6	5.73	41.6	114.8	7.33	31.9
rGCACG/d	19.2–31.4	0.27	0.26	0.27	44.5	126.8	5.18	41.3	116.5	6.50	27.6
rCAAUCG/d	10.5–23.7	0.77	0.77	0.77	58.9	177.9	3.76	50.0	147.6	5.97	21.6
rGGCACG/d	29.6–45.9	0.59	0.53	0.56	61.1	173.5	7.29	54.1	153.0	8.46	40.8
rCGUGCC/d	25.4–40.6	0.22	0.19	0.21	50.4	141.7	6.48	47.8	134.2	7.75	36.7
rGCACCG/d	20.5–47.6	0.37	0.27	0.32	56.4	159.0	7.08	51.9	148.3	7.70	40.0
rCGGUGC/d	27.7–42.7	0.86	0.84	0.85	51.2	142.1	7.11	40.9	108.8	8.45	40.5

Table 1. (Continued)

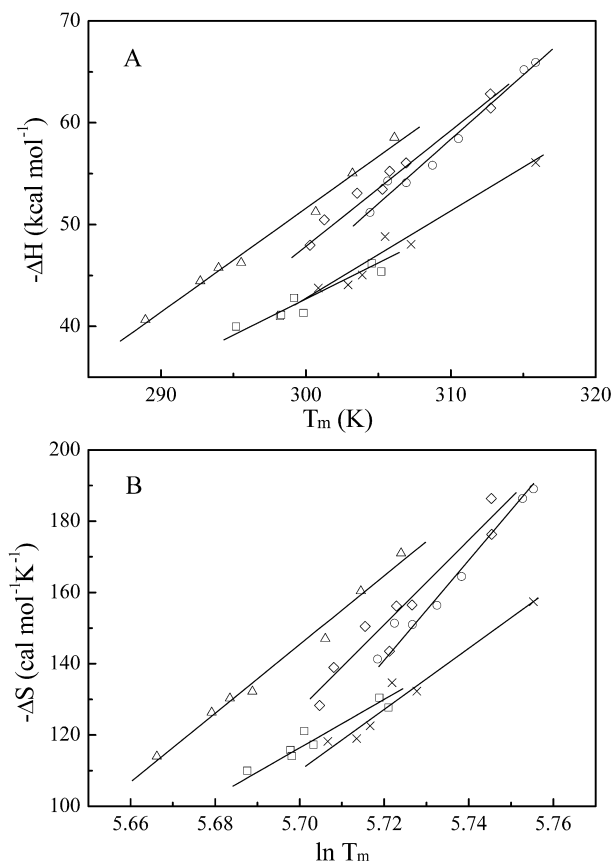|	Temperature range (°C)	Heat capacity change			Thermodynamic parameters at 37 °C			Thermodynamic parameters at 25 °C			T_m (°C)
		$-\Delta C_{p,H}$ (kcal·mol⁻¹·K⁻¹)	$-\Delta C_{p,S}$ (kcal·mol⁻¹·K⁻¹)	$-\Delta C_p^{ave}$ (kcal·mol⁻¹·K⁻¹)	$-\Delta H_{37}$ (kcal·mol⁻¹)	$-\Delta S_{37}$ (cal·mol⁻¹·K⁻¹)	$-\Delta G_{37}$ (kcal·mol⁻¹)	$-\Delta H_{25}$ (kcal·mol⁻¹)	$-\Delta S_{25}$ (cal·mol⁻¹·K⁻¹)	$-\Delta G_{25}$ (kcal·mol⁻¹)	
rGCCGUG/d	21.9–35.9	0.81	0.78	0.80	59.3	170.2	6.48	49.5	139.4	7.98	36.7
rCACGGC/d	23.2–41.7	0.95	0.89	0.92	52.4	146.0	7.16	41.1	111.0	7.98	40.7
rACGUAUG/d	15.8–33.0	1.02	0.96	0.99	61.9	181.2	5.76	49.7	143.1	7.05	33.1
rCGGUAUU/d	20.0–33.2	0.61	0.60	0.60	53.9	156.2	5.42	46.6	132.6	7.05	30.5
rAAUACCG/d	16.5–30.3	1.02	0.99	1.00	58.7	173.2	4.93	46.5	134.2	6.44	28.1
rUGAAGCU/d	28.6–40.2	1.10	1.06	1.08	59.7	171.2	6.62	46.5	129.5	7.93	37.5
rAGCUUCA/d	14.5–30.0	1.00	0.95	0.97	55.8	161.6	5.69	43.9	124.2	6.82	32.2
rCACGGCU/d	34.5–49.1	0.65	0.62	0.63	51.2	138.1	8.35	43.4	113.7	9.48	47.7
rAAUGUCGC/d	29.5–42.2	1.35	1.36	1.35	64.8	185.8	7.19	48.7	132.3	9.22	40.1
rGACUAGGU/d	30.7–48.2	0.69	0.67	0.68	59.3	165.4	8.04	51.0	139.1	9.57	44.8
rACCUAGUC/d	31.3–42.7	1.26	1.26	1.26	58.6	165.3	7.31	43.4	115.5	8.98	41.0
rCUAGUGGA/d	34.8–46.7	0.88	0.88	0.88	58.2	161.6	8.07	47.7	126.8	9.88	45.0
rGCCAGUUA/d	27.9–41.8	0.82	0.76	0.79	59.1	166.4	7.48	49.3	136.2	8.66	41.9
rUUACAGCG/d	26.9–40.6	1.13	1.16	1.15	55.7	158.1	6.63	42.1	112.3	8.61	37.6
rCGCUGUAA/d	29.8–37.1	1.89	1.89	1.89	67.1	196.1	6.31	44.5	121.5	8.25	36.0
rUUGGCACC/d	36.9–51.6	0.76	0.78	0.77	45.2	118.0	8.63	36.1	87.4	10.08	50.5
rCUACGCUU/d	20.7–35.6	0.59	0.58	0.58	56.1	160.0	6.49	49.0	137.3	8.07	36.8
rAAGCGUAG/d	31.6–45.0	0.66	0.69	0.68	60.9	171.7	7.63	52.9	144.3	9.91	42.6
rGAGCCGUG/d	40.0–56.0	1.36	1.33	1.34	52.3	139.3	9.12	36.0	86.9	10.13	50.7
rCACGGCUC/d	36.9–51.5	0.96	0.91	0.94	54.7	146.8	9.15	43.1	110.9	10.04	50.9
rACUGGAUU/d	31.9–42.8	0.38	0.36	0.37	59.0	166.4	7.40	54.5	152.1	9.11	41.6
rAAUCCAGU/d	21.5–36.0	0.58	0.62	0.60	49.0	139.2	5.82	42.1	114.9	7.80	32.5
rGGACUCAG/d	30.4–44.7	0.56	0.59	0.57	53.7	147.4	7.96	47.0	124.1	9.94	45.1
rCUGAGUCC/d	23.8–42.1	1.60	1.56	1.58	52.3	143.7	7.70	33.1	82.2	8.61	43.5
rGAGGUCGU/d	38.3–51.7	0.93	1.00	0.96	51.6	135.3	9.68	40.5	95.9	11.91	54.2
rACGACCUC/d	30.6–42.0	1.00	0.92	0.96	54.1	147.9	8.16	42.0	111.5	8.78	45.9
rAGUCCUGA/d	20.3–35.4	1.23	1.12	1.17	62.3	177.9	7.12	47.6	133.6	7.76	39.9
rGCCGUGAG/d	39.6–51.8	0.45	0.45	0.45	53.2	141.5	9.32	47.8	123.6	10.97	53.0
rCUUACGCU/d	23.6–36.9	1.58	1.60	1.59	59.8	172.7	6.20	40.8	109.7	8.04	35.2
rAUCUAUCCG/d	25.1–39.6	1.14	1.15	1.14	59.4	169.6	6.82	45.8	124.3	8.70	38.5
rCGCUGUUAG/d	33.8–44.6	0.38	0.50	0.44	61.5	172.7	7.93	56.9	152.9	11.29	44.0
rCAACAGCAA/d	31.0–48.3	1.07	1.07	1.07	44.5	117.5	8.02	31.6	75.4	9.10	46.6
rUUAACUGGC/d	37.6–52.0	1.38	1.28	1.33	65.6	185.0	8.25	49.1	134.4	9.05	44.7

Fig. 1. The representative temperature dependence of the thermodynamic parameters for various base-pair compositions. (A) ΔH vs. T_m; (B) ΔS vs. $\ln T_m$. rCGCUGUAA/dTTACAGCG (□), rCACGGCUC/dGAGCCGTG (×), rACCUAGUC/dGACTAGGT (△), rAGUCCUGA/dTCAGGACT (○), and rGAGCCGUG/dCACGGCTC (◇).

Fig. 2. The representative temperature dependence of the thermodynamic parameters for various base-pair lengths. (A) ΔH vs. T_m; (B) ΔS vs. $\ln T_m$. rAGCCG/dCGGCT (□), rCGGUGC/dGCACCG (×), rACGUAUG/dCATACGT (△), rACCUAGUC/dGACTAGGT (○), and rGUAACAGCG/dCGCTGTTAC (◇).

confirmed that the heat capacity changes derived from the spectroscopic and calorimetric measurements were in good agreement [54].

Temperature-dependent enthalpy and entropy changes

As the enthalpy and entropy changes are state functions, their values, in nature, are dependent on the temperature of interest. Table 1 summarizes the thermodynamic parameters of the 24 DNA/DNA and 41 RNA/DNA duplexes at standard temperature (25 °C) and physiological temperature (37 °C). Direct comparison shows that the temperature-independent and temperature-dependent thermodynamic parameters are clearly different, while the two mean values of the thermodynamic parameters derived from $\Delta C_P = 0$ and $\Delta C_P \neq 0$ are in excellent agreement (data not shown). These observations further support that the assumption of $\Delta C_P = 0$ would be more reasonable only when the statistical mean values of the thermodynamic parameters are taken into account.

To our knowledge, the published nearest-neighbor model parameters were generally extracted from the temperature-independent thermodynamic data of the oligonucleotide duplexes [16–25,57]. This requires that the melting tempera-

Fig. 3. Heat capacity change vs. the number of base pairs for DNA/DNA (○) and RNA/DNA (●) oligonucleotide duplexes.

tures of all the investigated sequences should have a small deviation from 37 °C over the experimental range. However, with the intrinsic limitation of the UV measurements, it is impossible to determine the thermodynamic parameters at the same temperature for all the duplexes only by

temperature-independent thermodynamic analysis. In other words, the experimental temperature range may be far lower than 37 °C for shorter oligonucleotide sequences or higher than 37 °C for longer oligonucleotide sequences. As a result, the simple extrapolation of the thermodynamic parameters to 37 °C is completely necessary. In this case, Eqns (6) and (7) provide a reasonable and valid way to estimate the thermodynamic parameters at the temperature of interest.

With the difference in detecting principles, the strand concentrations of the UV measurements are generally smaller than those of the DSC measurements for the same nucleotide sequences. Such differences in the strand concentration are rarely taken into account in the previous reports when the van't Hoff enthalpy changes were compared with the calorimetric enthalpy changes [30,31,33]. In fact, the melting temperature essentially depends on the strand concentration for a bimolecular transition. This implies that due to great different in the strand concentration, the van't Hoff enthalpy change derived from the temperature-independent thermodynamic analysis should be different from the calorimetric enthalpy change. If the two enthalpy changes were compared at the same temperature, the clear deviation would be cancelled. Recent studies have confirmed that there should be not statistically significant discrepancies in the enthalpy change when the heat capacity changes were taken into account [54,55]. As an alternative method, a plot of T_m^{-1} vs. $\ln(C_T/4)$ by combining the UV and DSC measurements was used [26].
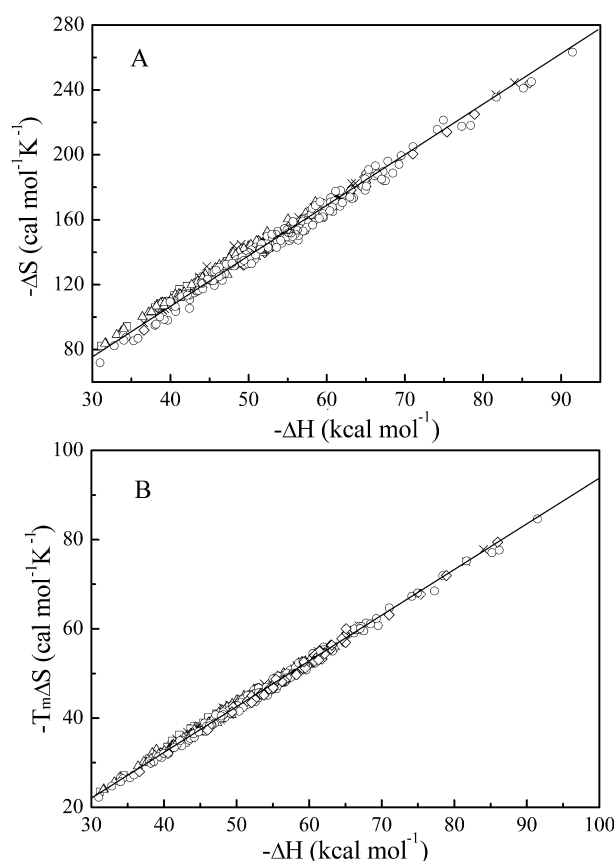
Enthalpy–entropy compensation

Figure 4 shows the compensation correlation of the temperature-dependent enthalpy and entropy changes for all the sequences listed in Table 1. Although a rectangular hyperbola relationship between the enthalpy and entropy changes was proposed [28,58], the plot in Fig. 4 is an approximate straight line [21,48,52,53,59]. The empirical correlation of the temperature-dependent enthalpy and entropy changes can be given by:

$$\Delta H = 0.983 \times T_m \Delta S - 8.218 \qquad (14)$$

where the correlation coefficient is 0.997 and the standard deviation is 0.734, respectively. This reflects the fact that the enthalpy–entropy compensation is significant and a large increase in the enthalpy change is necessarily accompanied by the large increase in the entropy change. Compared with the compensation of the temperature-independent enthalpy and entropy changes reported in a previous study ($\Delta H/T_m\Delta S = 1.15$ [48]), the extent of the compensation of the temperature-dependent enthalpy and entropy changes might be more significant.

The effects of heat capacity change on the free energy change and melting temperature

The free energy change and melting temperature are two critically important parameters, which are often used to characterize the stability of base pairing, to predict secondary or tertiary structures of nucleic acids, and to determine the optimal temperature in PCR, RCA, and *in situ* hybridization. In contrast to clear temperature-dependence of the enthalpy and entropy changes, the free energy change and melting temperature are relatively insensitive to the heat

Fig. 4. Compensation plot of temperature-dependent enthalpy and entropy for 5 bp (□), 6 bp (×), 7 bp (△), 8 bp (○), and 9 bp (◇). (A) A plot of ΔH vs. ΔS; (B) A plot of ΔH vs. $T_m\Delta S$. The straight lines were obtained by linear regression.

capacity change (data not shown). This suggests that the free energy change determined by $\Delta C_p = 0$ would be a more accurate parameter than either the individual enthalpy change or entropy change [13,21,39,52,53]. These observations have been confirmed by the DSC measurements, in which, despite an almost 100% difference in the two enthalpy changes for the investigated duplexes, the transition temperatures determined by the DSC measurements were in excellent agreement with the melting temperatures of the corresponding concentrations linearly extrapolated by the UV measurements [31].

The improved NN-model parameters

The nearest-neighbor model has been widely applied to predict the thermodynamic properties and secondary or tertiary structures of the sequence-dependent nucleotides [1–4,8]. In this model, the contribution of a given sequence to the thermodynamic properties is assumed to be directly related to the identity of the nearest-neighbor doublets and to have a linear dependence on the occurrence of these nearest neighbors [17,19,21,22,25,48,60,61]. Herein, we attempted to extract the NN-model free energy parameters at physiological temperature from the temperature-dependent thermodynamic data of the 41 RNA/DNA hybrids listed in Table 1 (see Table 2). As for the previous study

Table 2. Comparison of the NN-model free energy parameters at 37 °C for RNA/DNA hybrids. The temperature-independent free energy parameters were reported previously [19]. The temperature-dependent free energy parameters were extracted from the 41 RNA/DNA hybrids by the following equation: $\Delta G = \Delta G_{int} + \sum n_i \Delta G_i(NN)$, where ΔG_{int} is the initiation free energy, $\Delta G_i(NN)$ is the free energy change for the 16 possible Watson-Crick nearest neighbor base–pair interactions, and n_i is the occurrence number of the i-th nearest neighbor, respectively.

Sequences	Temperature-independent ΔG_{37} (kcal·mol^{-1})	Temperature-dependent ΔG_{37} (kcal·mol^{-1})
rAA/dTT	−1.0	−0.4
rAC/dTG	−2.1	−1.6
rAG/dTC	−1.8	−1.4
rAU/dTA	−0.9	−1.0
rCA/dGT	−0.9	−1.0
rCC/dGG	−2.1	−1.5
rCG/dGC	−1.7	−1.2
rCU/dGA	−0.9	−0.9
rGA/dCT	−1.3	−1.4
rGC/dCG	−2.7	−2.4
rGG/dCC	−2.9	−2.2
rGU/dCA	−1.1	−1.5
rUA/dAT	−0.6	−0.3
rUC/dAG	−1.5	−0.8
rUG/dAC	−1.6	−1.0
rUU/dAA	−0.2	−0.2
Initiation	3.1	1.0

[19], we find that the two NN-model free energy sets have nearly identical trends but there are clear differences for many nearest-neighbor sequences and helix initiation (see Table 2). Nevertheless, the mean values of 16 NN-model parameters determined by two different methods are similar (−1.5 kcal·mol^{-1} for $\Delta C_p = 0$ and −1.2 kcal·mol^{-1} for $\Delta C_p \neq 0$). A possible interpretation is that the two studies selected different oligonucleotide sequences and applied different thermodynamic analysis methods. As the thermodynamic parameters derived from $\Delta C_p = 0$ clearly depend on the experimental temperature range, it is impossible to determine the thermodynamic parameters at exactly 37 °C for all the investigated duplexes only by the temperature-independent thermodynamic analysis, thus small deviations in the free energy change of different sequences would accumulate and result in a large contribution to the NN-model parameters.

It should be noted that the published NN-model parameters were generally extracted from the temperature-independent thermodynamic data [17,19,21,22,25]. It is not surprising that some disagreement in the NN-model parameters has been revealed by several laboratories [17,20–22,57,62,63]. Although the unified NN-model parameters were suggested to be the salt concentration dependence of the oligonucleotide sequences [64], the heat capacity change would be an important factor [34,37–42,54,55]. Moreover, the primary results of Turner and coworkers confirmed that the NN-model parameter sets derived from the temperature-independent thermodynamics were somewhat different from those derived from the temperature-dependent thermodynamics [65]. Our work

extended their studies and extracted the NN-model free energy parameters from the temperature-dependent thermodynamic data. This improvement will enhance the accuracy of the predictions of the secondary or tertiary structures for nucleotide hybrids *in vivo*.

REFERENCES

1. Lück, R., Steger, G. & Riesner, D. (1996) Thermodynamic prediction of conserved secondary structure: application to the RRE element of HIV, the tRNA-like element of CMV and the mRNA of prion protein. *J. Mol. Biol.* **258**, 813–826.
2. Mathews, D.H., Sabina, J., Zuker, M. & Turner, D.H. (1999) Expanded sequence dependence of thermodynamic parameters improves prediction of RNA secondary structure. *J. Mol. Biol.* **288**, 911–940.
3. Zuker, M. (1989) On finding all suboptimal foldings of an RNA molecule. *Science* **244**, 48–52.
4. Chen, J.H., Le, S.Y. & Maizel, J.V. (2000) Prediction of common secondary structures of RNAs: a genetic algorithm approach. *Nucleic Acids Res.* **28**, 991–999.
5. Chee, M., Yang, R., Hubbel, E., Berno, A., Huang, X.H.C., Stern, D., Winkler, J., Lockhart, D.J., Morris, M.S. & Fodor, S.P. (1996) Accessing genetic information with high-density DNA arrays. *Science* **274**, 610–614.
6. Howell, W.M., Jobs, M., Gyllensten, U. & Brookes, A.J. (1999) Dynamic allele-specific hybridization. A new method for scoring single nucleotide polymorphisms. *Nat. Biotechnol.* **17**, 87–88.
7. Shi, G.Y. & Wu, H.L. (1988) Isolation and characterization of microplasminogen. A low molecular weight form of plasminogen. *J. Biol. Chem.* **263**, 17071–17075.
8. Lizardi, P.M., Huang, X., Zhu, Z., Bray-Ward, P., Thomas, D.C. & Ward, D.C. (1998) Mutation detection and single-molecule counting using isothermal rolling-circle amplification. *Nat. Genet.* **19**, 225–232.
9. Gibbs, R.A. (1990) DNA amplification by the polymerase chain reaction. *Anal. Chem.* **62**, 1202–1214.
10. Valenzuela, J.G., Francischetti, I.M.B. & Ribeiro, M.C. (1999) Purification, cloning, and synthesis of a novel salivary antithrombin from the mosquito *Anopheles albimanus*. *Biochemistry* **38**, 11209–11215.
11. Service, R.F. (1998) DNA chips survey an entire genome. *Science* **281**, 1122.
12. Marshall, A. & Hodgson, J. (1998) DNA chips: an array of possibilities. *Nat. Biotechnol.* **16**, 27–31.
13. SantaLucia, J. Jr & Turner, D.H. (1997) Measuring the thermodynamics of RNA secondary structure formation. *Biopolymers* **44**, 309–319.
14. Cooper, A. (1999) Thermodynamic analysis of biomolecular interactions. *Curr. Opin. Chem. Biol.* **3**, 557–563.
15. Freire, E. (1995) Thermal denaturation methods in the study of protein folding. *Methods Enzymol.* **259**, 144–168.
16. Freier, S.M., Kierzek, R., Jaeger. J.A., Sugimoto, N., Caruthers, M.H., Neilson, T. & Turner, D.H. (1986) Improved free-energy parameters for predictions of RNA duplex stability. *Proc. Natl Acad. Sci. USA* **83**, 9373–9377.
17. Breslauer, K.J., Frank, R., Blocker, H. & Marky, L.A. (1986) Predicting DNA duplex stability from the base sequence. *Proc. Natl Acad. Sci. USA* **83**, 3746–3750.

18. Walter, A.E. & Turner, D.H. (1994) Sequence dependence of stability for coaxial stacking of RNA helixes with Watson–Crick base paired interfaces. *Biochemistry* **33**, 12715–12719.

19. Sugimoto, N., Nakano, S., Katoh, M., Matsumura, A., Nakamuta, H., Ohmichi, T., Yoneyama, M. & Sasaki, M. (1995) Thermodynamic parameters to predict stability of RNA/DNA hybrid duplexes. *Biochemistry* **34**, 11211–11216.

20. Sugimoto, N., Nakano, S., Yoneyama, M. & Honda, K. (1996) Improved thermodynamic parameters and helix initiation factor to predict stability of DNA duplexes. *Nucleic Acids Res.* **24**, 4501–4505.

21. Allawi, H. & SantaLucia, J. Jr (1997) Thermodynamics and NMR of internal G·T mismatches in DNA. *Biochemistry* **36**, 10581–10594.

22. Xia, T., SantaLucia, J. Jr, Burkard, M.E., Kierzek, R., Schroeder, S.J., Jiao, X., Cox, C. & Turner, D.H. (1998) Thermodynamic parameters for an expanded nearest-neighbor model for formation of RNA duplexes with Watson–Crick base pairs. *Biochemistry* **37**, 14719–14735.

23. Bommarito, S., Peyret, N. & SantaLucia, J. Jr (2000) Thermo-dynamic parameters for DNA sequences with dangling ends. *Nucleic Acids Res.* **28**, 1929–1934.

24. Sugimoto, N., Nakano, M. & Nakano, S. (2000) Thermo-dynamics–structure relationship of single mismatches in RNA/DNA duplexes. *Biochemistry* **39**, 11270–11281.

25. Chen, X., Kierzek, R. & Turner, D.H. (2001) Stability and structure of RNA duplexes containing isoguanosine and iso-cytidine. *J. Am. Chem. Soc.* **123**, 1267–1274.

26. Jelesarov, I., Crane-Robinson, C. & Privalov, P.L. (1999) The energetics of HMG box interactions with DNA: thermodynamic description of the target DNA duplexes. *J. Mol. Biol.* **294**, 981–995.

27. Holbrook, J.A., Capp, M.W., Saecker, R.M. & Record, M.T. Jr (1999) Enthalpy and heat capacity changes for formation of an oligomeric DNA duplex: interpretation in terms of coupled pro-cesses of formation and association of single-stranded helices. *Biochemistry* **38**, 8409–8422.

28. Rouzina, I. & Bloomfield, V.A. (1999) Heat capacity effects on the melting of DNA. 1. General aspects. *Biophys. J.* **77**, 3242–3251.

29. Rouzina, I. & Bloomfield, V.A. (1999) Heat capacity effects on the melting of DNA. 2. Analysis of nearest-neighbor base pair effects. *Biophys. J.* **77**, 3252–3255.

30. Wu, P. & Sugimoto, N. (2000) Transition characteristics and thermodynamic analysis of DNA duplex formation: a quantitative consideration for the extent of duplex association. *Nucleic Acids Res.* **28**, 4762–4768.

31. Vallone, P.M. & Benight, A.S. (2000) Thermodynamic, spectro-scopic, and equilibrium binding studies of DNA sequence context effects in four 40 base pair deoxyoligonucleotides. *Biochemistry* **39**, 7835–7846.

32. Vesnaver, G., Chang, C.N., Eisenberg, M., Grollman, A.P. & Breslauer, K.J. (1989) Influence of abasic and anucleosidic sites on the stability, conformation, and melting behavior of a DNA duplex: correlations of thermodynamic and structural data. *Proc. Natl Acad. Sci. USA* **86**, 3614–3618.

33. Riccelli, P.V., Vallone, P.M., Kashin, I., Faldasz, B.D., Lane, M.J. & Benight, A.S. (1999) Thermodynamic, spectroscopic, and equilibrium binding studies of DNA sequence context effects in six 22-base pair deoxyoligonucleotides. *Biochemistry* **38**, 11197–11208.

34. Naghibi, H., Tamura, A. & Sturtevant, J.M. (1995) Significant discrepancies between van't Hoff and calorimetric enthalpies. *Proc. Natl. Acad. Sci. USA* **92**, 5597–5599.

35. Sugimoto, N., Wu, P., Hara, H. & Kawamoto, Y. (2001) pH and cation effects on the properties of parallel pyrimidine motif DNA triplexes. *Biochemistry* **40**, 9396–9405.

36. Chalikian, T.V., Völker, J., Plum, G.E. & Breslauer, K.J. (1999) A more unified picture for the thermodynamics of nucleic acid duplex melting: a characterization by calorimetric and volume tric techniques. *Proc. Natl Acad. Sci. USA* **96**, 7853–7858.

37. Liu, Y. & Sturtevant, J.M. (1997) Significant discrepancies between van't Hoff and calorimetric enthalpies. *Biophys. Chem.* **64**, 121–126.

38. Chaires, J.B. (1997) Possible origin of differences between van't Hoff and calorimetric enthalpy estimates. *Biophys. Chem.* **64**, 15–23.

39. Petersheim, M. & Turner, D.H. (1983) Base-stacking and base-pairing contributions to helix stability: thermodynamics of double-helix formation with CCGG, CCGGp, CCGGAp, CCGGUp, and ACCGGUp. *Biochemistry* **22**, 256–263.

40. Freier, S.M., Burger, B.J., Alkema, D., Neilson, T. & Turner, D.H. (1983) Effects of 3′ dangling end stacking on the stability of GGCC and CCGG double helices. *Biochemistry* **22**, 6198–6206.

41. Freier, S.M., Alkema, D., Sinclair, A., Neilson, T. & Turner, D.H. (1985) Contributions of dangling end stacking and terminal base-pair formation to the stabilities of XGGCCp, XCCGGp, XGGCCYp, and XCCGGYp helixes. *Biochemistry* **24**, 4533–4539.

42. Kierzek, R., Caruthers, M.H., Longfellow, C.E., Swinton, D., Turner, D.H. & Freier, S.M. (1986) Polymer-supported RNA synthesis and its application to test the nearest-neighbor model for duplex stability. *Biochemistry* **25**, 7840–7846.

43. Rentzeperis, D., Ho. J. & Marky, L.A. (1993) Contribution of loops and nicks to the formation of DNA dumbbells: melting behavior and ligand binding. *Biochemistry* **32**, 2564–2572.

44. Longfellow, C.E., Kierzek, R. & Turner, D.H. (1990) Thermo-dynamic and spectroscopic study of bulge loops in oligor-ibonucleotides. *Biochemistry* **29**, 278–285.

45. Evertsz, E.M., Rippe, K. & Jovin, T.M. (1994) Parallel-stranded duplex DNA containing blocks of *trans* purine-purine and purine-pyrimidine base pairs. *Nucleic Acids Res.* **22**, 3293–3303.

46. McDowell, J.A. & Turner, D.H. (1996) Investigation of the structural basis for thermodynamic stabilities of tandem GU mismatches: solution structure of (rGAG*GU*CUC) $_2$ by two-dimensional NMR and simulated annealing. *Biochemistry* **35**, 14077–14089.

47. Ratilainen, T., Holmen, A., Tuite, E., Nielsen, P.E. & Norden, B. (2000) Thermodynamics of sequence-specific binding of PNA to DNA. *Biochemistry* **39**, 7781–7791.

48. Nakano, S., Fujimoto, M., Hara, H. & Sugimoto, N. (1999) Nucleic acid duplex stability: influence of base composition on cation effects. *Nucleic Acids Res.* **27**, 2957–2965.

49. Makhatadze, G.I. & Privalov, P.L. (1990) Heat capacity of proteins. I. Partial molar heat capacity of individual amino acid residues in aqueous solution: hydration effect. *J. Mol. Biol.* **213**, 375–384.

50. Privalov, P.L. & Makhatadze, G.I. (1992) Contribution of hydration and non–covalent interactions to the heat capacity effect on protein unfolding. *J. Mol. Biol.* **224**, 715–723.

51. Spolar, R.S., Livingstone, J.R. & Record, M.T. Jr (1992) Use of liquid hydrocarbon and amide transfer data to estimate con-tributions to thermodynamic functions of protein folding from the removal of nonpolar and polar surface from water. *Biochemistry* **31**, 3947–3955.

52. Sigurskjold, B.W. & Bundle, D.R. (1992) Thermodynamics of oligosaccharide binding to a monoclonal antibody specific for a Salmonella O-antigen point to hydrophobic interactions in the binding site. *J. Biol. Chem.* **267**, 8371–8376.

53. McPhail, D. & Cooper, A. (1997) Thermodynamics and kinetics of dissociation of ligand-induced dimers of vancomycin anti-biotics. *J. Chem. Soc. Faraday Trans.* **93**, 2283–2289.

54. Horn, J.R., Russell, D., Lewis, E.A. & Murphy, K.P. (2001) van't Hoff and calorimetric enthalpies from isothermal titration calori-

metry: are there significant discrepancies? *Biochemistry* **40**, 1774–1778.

55. Diamond, J.M., Turner, D.H. & Mathews, D.H. (2001) Thermodynamics of three-way multibranch loops in RNA. *Biochemistry* **40**, 6971–6981.

56. Barnes, T.W. III & Turner, D.H. (2001) Long-range cooperativity in molecular recognition of RNA by oligodeoxynucleotides with multiple C5-(1-propynyl) pyrimidines. *J. Am. Chem. Soc.* **123**, 4107–4118.

57. SantaLucia, J. Jr, Allawi, H. & Seneviratne, P.A. (1996) Improved nearest-neighbor parameters for predicting DNA duplex stability. *Biochemistry* **35**, 3555–3562.

58. Petruska, J. & Goodman, M.F. (1995) Enthalpy-entropy compensation in DNA melting thermodynamics. *J. Biol. Chem.* **270**, 746–750.

59. SantaLucia, J. Jr, Kierzek, R. & Turner, D.H. (1991) Functional group substitutions as probes of hydrogen bonding between GA mismatches in RNA internal loops. *J. Am. Chem. Soc.* **113**, 4313–4322.

60. Crothers, D.M. & Zimm, B.H. (1964) Theory of the melting transition of synthetic polynucleotides: evaluation of the stacking free energy. *J. Mol. Biol.* **9**, 1–9.

61. Ohmichi, T., Nakamuta, H., Yasuda, K. & Sugimoto, N. (2000) Kinetic property of bulged helix formation: analysis of kinetic behavior using nearest-neighbor parameters. *J. Am. Chem. Soc.* **122**, 11286–11294.

62. Borer, P.N., Dengler, B., Tinoco, I. Jr & Uhlenbeck, O.C. (1974) Stability of ribonucleic acid double-stranded helices. *J. Mol. Biol.* **86**, 843–853.

63. Doktycz, M.J., Goldstein, R.F., Paner, T.M., Gallo, F.J. & Benight, A.S. (1992) Studies of DNA dumbbells. I. Melting curves of 17 DNA dumbbells with different duplex stem sequences linked by T4 endloops: evaluation of the nearest–neighbor stacking interactions in DNA. *Biopolymers* **32**, 849–864.

64. SantaLucia, J. Jr (1998) A unified view of polymer, dumbbell, and oligonucleotide DNA nearest-neighbor thermodynamics. *Proc. Natl. Acad. Sci. USA* **95**, 1460–1465.

65. Freier, S.M., Sinclair, A., Neilson, T. & Turner, D.H. (1985) Improved free energies for G·C base-pairs. *J. Mol. Biol.* **185**, 645–647.

SUPPLEMENTARY MATERIAL

The following material is available from http://www.blackwell-science.com/products/journals/suppmat/EJB/EJB2970/EJB2970sm.htm

Detailed derivations of Eqns (11) and (12).

Table S1. Temperature-independent thermodynamic parameters of DNA complexes.

Table S2. Direct comparison of temperature-independent and temperature-dependent thermodynamic parameters for DNA complexes

Table S3. Mean values of the fitted thermodynamic parameters derived from $\Delta C_P = 0$ and $\Delta C_P \neq 0$.